

physica **p** status **s** solidi **S**

www.interscience.wiley.com

reprints

physica status solidi ^a
www.pss-a.com
applications and materials science
Editor's Choice
Highly efficient all-nitride phosphor-converted white light emitting diode
(Regina Mueller-Mach et al., p. 1727)
WILEY-VCH
www.pss-a.com

physica status solidi ^b
www.pss-b.com
basic solid state physics
Current Trends in Electronic Structure: Embedding and Linear Scaling Techniques
Thomas Beck, and Eduardo Hernandez
SPECIAL ISSUE
www.pss-b.com

physica status solidi ^c
[www.pss-c.com
current topics in solid state physics
Resonance feedback color center lasers in wide band gap materials excited by a pair of chirped femtosecond pulses
\(Anderson et al., p. 637\)
\[www.pss-c.com\]\(http://www.pss-c.com\)](http://www.pss-c.com)

physica status solidi ^r
www.pss-rapid.com
rapid research letters
Isolated trap
Crystal
www.pss-rapid.com

Thermoluminescence assessment of 0.5, 1.0 and 4.0 μm thick HFCVD undoped diamond films

R. Meléndrez¹, V. Chernov¹, P. W. May², B. Castañeda³, M. Pedroza-Montero¹, and M. Barboza-Flores^{*,1}

¹ Centro de Investigación en Física, Universidad de Sonora, A. P. 5-088, Hermosillo 83190, Sonora, México

² School of Chemistry, University of Bristol, Bristol, BS8 1TS, UK

³ Departamento de Investigación en Física, Universidad de Sonora, Hermosillo 83190, Sonora, México

Received 2 April 2009, revised 18 May 2009, accepted 20 May 2009

Published online 21 August 2009

PACS 78.60.Kn, 81.05.Uw, 81.15.Gh

* Corresponding author: e-mail mbarboza@cajeme.cifus.uson.mx, Phone: 55 662259 2156, Fax: 55 662212 6649

Chemical vapor deposition (CVD) diamond has not found extensive application as a thermoluminescence (TL) dosimeter, mainly because its TL glow curve shape is not reproducible. A slight variation in the growing conditions may result in strong changes in the morphology, microstructure, and surface-impurity-related defects, considerably affecting the TL glow curve features. In order to study the main TL characteristics under controlled growing conditions, we present results on three 0.5, 1.0, and 4.0 μm thick hot filament CVD (HFCVD) diamond films grown on Si (100) substrates. The recorded TL glow curves were resolved into individual peaks by a home-made deconvolution program and the kinetic parameters of the peaks were

extracted. The best fits of the TL glow curves were obtained using four peaks, except for the 4.0 μm thick sample that required five TL components. All samples showed three high intensity TL peaks between 180–400 °C and a less intense one or two peaks in the 100–180 °C low-temperature region. The low-temperature components all obey second-order kinetics while the high-temperature ones obey first and 1.6 order kinetics. The samples showed similar TL peaks with comparable kinetics parameters. It is concluded that the manufacturing of high quality HFCVD diamond may require a further improvement in the growing process in order to exploit its excellent tissue-equivalence properties in clinical and medical applications.

© 2009 WILEY-VCH Verlag GmbH & Co. KGaA, Weinheim

1 Introduction Thermoluminescence (TL) is usually observed in chemical vapor deposition (CVD) diamond samples that were previously exposed to ionizing radiation. After heating the specimen above the temperature at which the irradiation was carried out, the light emission intensity measured as a function of temperature provides a distinctive TL glow curve. The glow curve gives information regarding the charge trapping and transfer processes resulting in radiative recombination [1]. Localized trapping levels or traps in diamond may be formed inside the wide (5.5 eV) band gap by impurities, doping materials or defects. On the other hand, the CVD diamond growing conditions may have a strong effect on the morphological properties, crystalline structure, grain boundaries and defect concentration, affecting the number, and distribution of the trap energy levels in CVD diamond films. Therefore, the TL glow curve shape and peak structure depend strongly on the growth conditions and existing defects in the CVD diamond, making the TL phenomenon a relatively complex process to understand and replicate for TL dosimetry (TLD) applications.

TL detection and dose assessment of many types of ionizing and non-ionizing radiation applications using synthetic diamond grown by CVD depends on having reproducible TL properties and dose response. Unfortunately, the CVD diamond films produced in different laboratories have not shown standard TL properties [2–10], which is a serious disadvantage in comparison to the current TLD materials like LiF:Mg, Ti; LiF:Mg, Cu, P; and Al₂O₃:C. In the present work, we studied the TL properties of three undoped diamond films grown by hot filament CVD by utilizing identical growth conditions and growth rates $\approx 0.5 \mu\text{m}/\text{h}$. All films were grown on Si (100) substrates having an estimated 0.5, 1.0, and 4.0 μm thicknesses for 1.5, 4.0, and 8 h growth times, respectively. They were labeled A1, A2, and A3 as depicted in Table 1. The aim of this work was to perform a TL characterization and to determine the kinetic parameters associated with shallow and deep traps in these CVD diamond films. TL is an excellent method for testing the homogeneity of the CVD layer linked to defects, impurity content, morphology, and microstructure.

Table 1 Characteristics of HFCVD diamond films.

sample	growth time (h)	estimated thickness (μm)
A1	1.5	0.5
A2	4.0	1.0
A3	8.0	4.0

2 Experimental The hot filament CVD diamond films were grown on Si (100) boron-doped $5 \times 5 \text{ mm}^2$ (resistivity 1–100 Ω) substrates by using a 1% CH_4/H_2 gas mixture and growth rates $\approx 0.5 \mu\text{m/h}$. The diamond samples were β -irradiated using a ^{90}Sr – ^{90}Y source having an activity of 0.04 Ci and 5 Gy/min dose rate. The CVD diamond quality and surface morphology were assessed by Raman and scanning electron microscopy (SEM) techniques, respectively. The TL measurements were carried out on an automated Risø TL/OSL reader (model TL/OSL–DA-15) and heating rate of 2°C/s .

3 Results and discussions Raman spectroscopy allows for ready identification of the typical sharp line at 1332 cm^{-1} associated with the first-order phonon mode for diamond, which is characteristic of good quality diamond. Raman spectroscopy is known to be an ideal and non-destructive tool to differentiate between all the forms of crystalline and amorphous carbons, either in the sp^2 or sp^3 configuration. The 1332 cm^{-1} band is depicted in Fig. 1 for the three CVD diamond samples showing a systematic intensity increase as the growth time increases. The Raman spectra indicate the high quality of the diamond films. The A1 film also shows a low intensity broad absorption between 1480 and 1580 cm^{-1} , not observed in the A2 and A3 samples, indicating that there may be a small amount of graphitic or amorphous carbon present in the film. Raman spectroscopy may provide information from phase

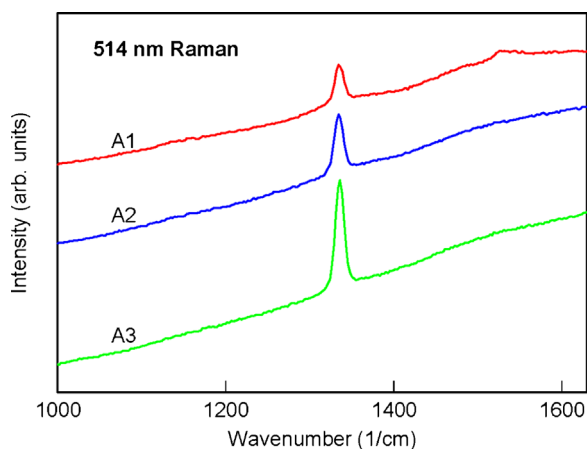


Figure 1 (online colour at: www.pss-a.com) Raman spectra of CVD diamond films using 514 nm excitation. The codes A1–3 are explained in Table 1.

purity to crystal perfection, to occurrence of impurities and extended defects, which are very important for tailoring the thermally stimulated luminescence properties of diamond films adequate for TLD applications. The structural defects and impurities decrease the crystalline perfection of diamond films and create states within the diamond band gap, which give rise to localized trapping levels in CVD diamond films.

Complementary information about the diamond film surface morphology and the growth time was investigated by SEM. Figure 2 shows the micrographs of the diamond film surfaces. The films are composed of sharp well-faceted micro-crystallites ranging in size from about 0.1 to $2 \mu\text{m}$ with many twinned crystallites. They have no evident preferential orientation and the crystal size depended on the growth time. Film A1 exhibited an inhomogeneous surface growth and smaller size crystallite distribution. This microstructural characteristic may be associated to the observed low intensity 1332 cm^{-1} diamond Raman band and the peaks around 1480 – 1580 cm^{-1} . The A2 and A3 diamond samples micrographs shows well-faceted micro-crystallites ranging in size from about 0.5 to $2 \mu\text{m}$ characteristic of a continuous film with well-defined facets composed mainly of diamond, as indicated by its Raman spectrum, and very little non-diamond component. The growth of good quality CVD diamond films involves, first, nucleation of individual crystallites on the substrate surface, then three-dimensional growth of these crystallites, faceting and coalescence with neighboring crystallites, and finally growth of a continuous polycrystalline diamond layer. This growth process is very likely happening as depicted by series of SEM micrographs showed: in the A1 sample the growth time was too short to produce a continuous diamond film, whereas in A2 and A3 the films had coalesced.

TL characterization was carried out using a home-made deconvolution program based on the non-linear least-square Marquardt method from which the kinetic parameters were extracted. The curve-fitting method, described in detailed elsewhere [10], was performed to obtain the best fit to experimental data, assuming a given number of general order kinetics peaks. Therefore, the best fit provided the kinetic order and values for the activation energy E (eV) and frequency factor s (s^{-1}). The best fits are shown in Figs. 3–5 and the values of the kinetic parameters are shown in Tables 2–4.

The TL glow curve shapes in all samples are characterized by a dominant TL peak around 250 – 300°C and a less intense peak in the 100 – 145°C low-temperature region. The low-temperature components all obey second-order kinetics and are located around 100 – 145°C . The dominant TL peaks are of first-order kinetics except for sample A3 that obeys kinetics order of ~ 1.6 . It should be recalled that a first-order kinetics process means negligible retrapping during the thermal stimulation, and is characterized by an asymmetric TL peak being wider on the low temperature side than on the high temperature side, a feature clearly shown in Figs. 3–5. In contrast, a second-order TL peak is wider and more symmetric

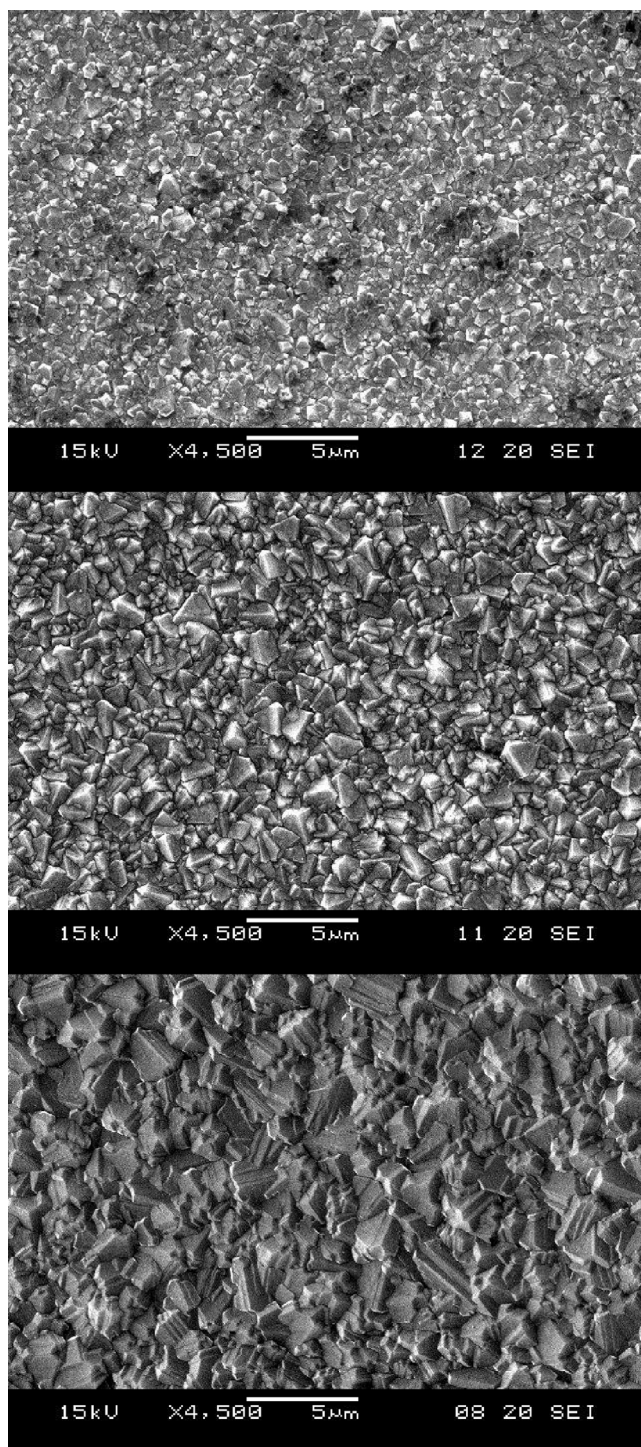


Figure 2 Typical SEM micrographs of A1 (top), A2 (middle), and A3 (bottom) CVD diamond films.

than a first-order peak. Physically, this means that a significant part of the released charge carriers are retrapped before they recombine, giving rise to a spreading bell-shaped TL emission over a wider temperature range, as seen in peak 1 of samples A1 and A2, and peaks 1 and 2 of sample A3.

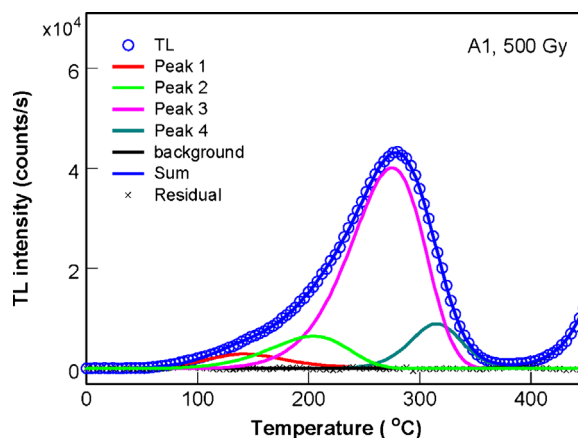


Figure 3 (online colour at: www.pss-a.com) TL glow curve of A1 CVD diamond film (circles) deconvoluted into separate peaks (thin lines) with the kinetic parameters presented in Table 2. The blue line is the sum of the peaks and the background.

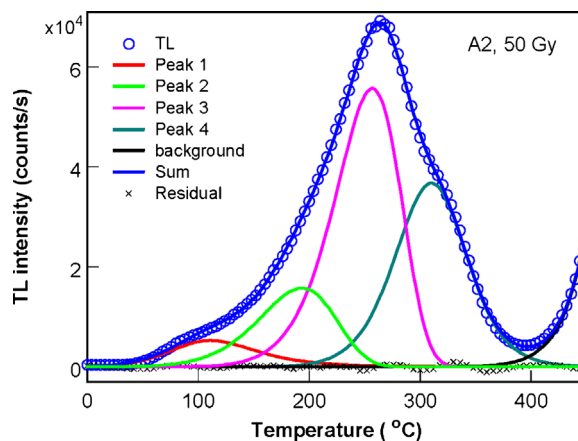


Figure 4 (online colour at: www.pss-a.com) TL glow curve of A2 CVD diamond film (circles) deconvoluted into separate peaks (thin lines) with the kinetic parameters presented in Table 3. The blue line is the sum of the peaks and the background.

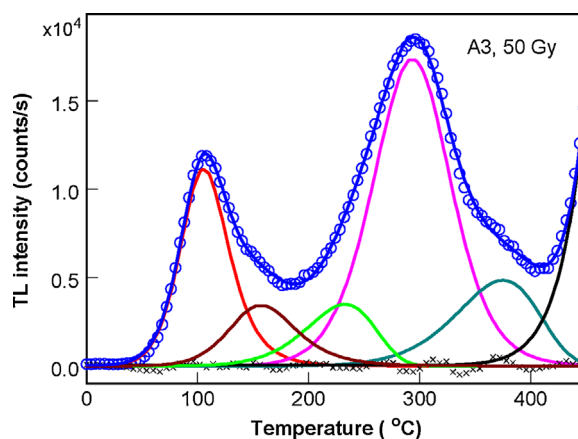


Figure 5 (online colour at: www.pss-a.com) TL glow curve of A3 CVD diamond film (circles) deconvoluted into separate peaks (thin lines) with the kinetic parameters presented in Table 4. The blue line is the sum of the peaks and the background.

Table 2 Kinetic parameters for A1 CVD diamond film.

peak	temperature of maximum (°C)	kinetic order	activation energy (eV)	frequency factor (s ⁻¹)
1	143	2	0.55	3.3×10^5
2	203	1	0.53	2.2×10^4
3	274	1	0.74	3.7×10^5
4	315	1.6	1.61	7.2×10^{12}

Table 3 Kinetic parameters for A2 CVD diamond film.

peak	temperature of maximum (°C)	kinetic order	activation energy (eV)	frequency factor (s ⁻¹)
1	114	2	0.43	2.3×10^4
2	192	1	0.51	1.8×10^4
3	256	1	0.78	2.1×10^6
4	311	1.6	1.12	3.5×10^8

Table 4 Kinetic parameters for A3 CVD diamond film.

peak	temperature of maximum (°C)	kinetics order	activation energy (eV)	frequency factor (s ⁻¹)
1	106	2	0.78	2.9×10^9
2	159	2	0.72	2.3×10^7
3	232	1	0.68	3.7×10^5
4	294	1.6	0.97	2.9×10^7
5	374	1	0.93	8.5×10^5

Several studies have shown that CVD diamond films exhibit very different TL glow peak structures depending on their growth parameters, impurities, and doping materials. Since TL is very sensitive to defects and impurity-related centers, it is a difficult task to assign a TL glow peak to a particular impurity or defect. However, the glow curve shape for most synthetic CVD diamonds seems to be composed of one or two main bands peaked at 50–150 and 200–350 °C, along with some overlapped structure of different intensities TL peaks [2–15]. The TLD performance of CVD diamond has been tested in a number of diamond samples of diverse origin. For example, a batch of 20 CVD diamond samples from the same wafer, from Institute of Material Research at Limburg University, Belgium, showed a non-reproducible 30% discrepancy TL response without previous annealing [5, 8]. The TL variations and fluctuation diminished after 1 h annealing at 400 °C before irradiation. The TL variations were attributed to a non-homogeneous distribution of dopant concentration across the CVD wafer from which the examined samples came. Other authors investigated the TL properties of ten CVD diamond specimens and found around 5% TL reproducibility and sensitivity comparable to commercial LiF dosimeters, although no batch homogeneity was reported [16, 17]. Six high-quality CVD diamond cut from the same wafer obtained from De Beers Industrial

Diamonds (UK) Ltd. exhibited a 2% reproducibility over ten TL measurements and an average of 6.1% for the six samples [3]. A more recent comparative investigation on the TL properties focused on clinical dosimetry, established 3% TL measurement reproducibility on 20 CVD diamond samples synthesized by the Naval Research Laboratory. The samples showed a remarkable $\pm 5\%$ TL sensitivity from the mean value, which was five times higher than that of the commercially available TLD 100 dosimeter [18]. It is to be noted that some of the large 2–30% reproducibility differences may be due to the TL read-out protocols used, annealing conditions as well as local environmental disturbance. There is a general agreement that TL glow curve features and dosimetry performance originates from the CVD diamond crystallographic defects and centers as a result of extrinsic substitutional impurities or intrinsic-like interstitials introduced during the growth process.

The effect of nitrogen incorporation in CVD diamond films during growth on the TL performance has been undertaken with the expectation that this may control the trapping level population to improve the TL sensitivity, reproducibility, and dose linearity [19–21]. Indeed, optimization of the TL intensity and dose linearity were found through incorporation of 20 ppm nitrogen concentration in the gas phase [20]. However, the TL glow curve had different shapes depending on nitrogen concentration. The low-temperature peak, clearly observed for low or zero nitrogen incorporation, decreased for higher nitrogen concentration. In addition, the high-temperature peak shifted from 230 to 250 °C when the nitrogen concentration incorporated into the diamond film increased, except for a nitrogen concentration of 20 ppm where the peak position remained at 230 °C. Also, a 20 ppm nitrogen concentration increased the TL dose saturation region from about 1 Gy (undoped) to about 40 Gy, which is a remarkable improvement with respect to undoped diamond samples. Further studies in the same set of samples using micro-Raman spectroscopy and secondary ion mass spectroscopy identified the contribution of graphitic phases and DLC or amorphous carbon for samples with a 2% [N₂/H₂] concentration in the gas phase [21]. The nitrogen luminescence bands corresponding to an interstitial nitrogen atom bonded to the nearest vacancy and to the NV system (vacancy trapped at a substitutional nitrogen atom) were identified. A significant finding established from the same work [21] was that shallow levels, corresponding to near-room-temperature peaks, were associated with low nitrogen incorporation, while the high-temperature peak, corresponding to deep levels were characteristic of higher nitrogen incorporation samples.

The relative TL glow curve peak intensities and shifting of its temperature maxima as a function of incorporated nitrogen concentration has also been observed in nominally pure CVD samples in which no nitrogen has been incorporated [19]. The films were unintentionally contaminated with nitrogen from air leaks or impurities in reactants. However, nitrogen concentrations were estimated to be in the range of 5–26 ppm, producing a TL increase in the low-temperature

peak, optimized around 10 ppm, along with a TL intensity decrease in the rest of the observed TL peaks as the nitrogen concentration increased. Therefore, even traces or extremely low nitrogen doping levels, may cause strong effects on the TL glow curve shape modifying the population and trapping-level distribution in CVD diamond films. Boron-doped CVD diamond films enhance around 25% the TL sensitivity in concentrations below 15 ppm with respect to undoped samples. However, for higher boron concentrations (>15 ppm) the high-temperature glow peaks decrease drastically and low-temperature peak component appears around 70 °C [22].

It should be recalled that the main consequence of nitrogen or boron incorporation is to change the morphology and defect content of the films [23, 24], which are responsible for the thermally stimulated luminescence (TL), current (TSC), and exoelectronic emission (TSEE) associated with defect formation during growing and localized levels within the gap [25, 26]. The presence of structural defects and compositional impurities, which, of course, depend on the growth conditions, strongly affects the charge transport, collection efficiency and trapping population, and causes evident effects on the TL glow curve. It is also important to stress the fact that even traces of nitrogen or boron impurities may have a strong effect on the morphology and defect formation on the CVD diamond samples. Therefore, the TL glow curves shown in Figs. 3–5 may contain different nitrogen (or boron) features linked to nitrogen-related defects with changing morphology characteristics as the growth time increases.

The high-intensity TL glow peak around 250–300 °C observed in the CVD diamond samples shown in Figs. 3–5 has also been observed by other authors, but peaked at around 267 [2, 11, 18, 30], 247 [19, 21], and 287 °C [21] overlapped by a broad spectral TL 400–600 nm emission band attributed to the well-known A-band associated with donor–acceptor recombination pairs [22], where the donor would be nitrogen and the acceptor boron [19]. The A-band has been observed in natural and synthetic diamond as a broad 590–413 nm band [27]. The glow peak components with their activation energies are shown in Tables 2–4, and are in agreement with previously reported data. The differences may be accounted for by the particular TL read-out protocol or the glow curve deconvolution used. Although some TL glow peaks have been ascribed to the presence of nitrogen or boron, additional investigation is required due to the complexity of defects and center formation.

The detection of defects and centers requires the use of high resolution spectroscopic techniques, like photoluminescence (PL), cathodoluminescence (CL), or ion beam induced luminescence (IBIL), which may provide conclusive identification of the luminescence from defects and centers in CVD diamond films. At the moment, we have no spectroscopic information about the samples investigated here, and work on this is in progress. However, we have performed a very detailed IBIL on several CVD diamond samples that indicates the presence of different nitrogen-vacancy complexes, even in high-quality nominally undoped

CVD diamond films [27]. Nitrogen-vacancy center emissions corresponding to $[N_s-V-N_s]^0$, $[N_s-V]^0$, $[N-V]^n$, and $[N-V]^-$ were found in HFCVD and microwave CVD (MWCVD) diamond film specimens [27–31]. The spectrally resolved TL glow curve, *i.e.*, the TL intensity as a function of emission wavelength and temperature, may provide information about the impurities, defects, and radiative recombination centers in a CVD diamond film, although with less sensitivity than IBIL [18, 21, 27]. Therefore, the standard TL glow curve, recorded as a TL intensity-temperature curve, has a strong limitation for the identification of defects and centers. However, as the CVD growth process improves its control on impurities and morphological features of the deposited films, the TL glow curve might become a genuine signature of the quality of CVD diamond films.

4 Conclusions Synthetic diamond grown by CVD is a very attractive material for TLD applications. In spite of the large potentialities, like having soft-tissue equivalence, chemical stability, and non-toxicity, the growth of CVD diamond films with tailored TL properties for radiation dosimetry has been a difficult goal to achieve. The reason is the great number of defects and centers created during growth by impurities materials and instabilities of the CVD reactor parameters. The presence of structural defects and compositional impurities, which depend on the growth conditions, strongly affect the TL response of the CVD diamond film. We have provided evidence that the TL glow curve features change as a function of growth time of high-quality HFCVD diamond films grown under the same reactor conditions. In spite of the strict control on the growth and precursor gas conditions imposed in the present experiment, we found no obvious correlation between the growth conditions and the TL pattern. This may perhaps be due to the HFCVD method used, which may produce a great variety of defect complexes responsible for the irregular TL glow curve features. It is expected that the MWCVD technique would provide CVD diamond samples with a more systematic TL behavior. The TL glow curve structure may be ascribed to nitrogen-vacancy complexes caused by traces of nitrogen or other contaminants that modifies film morphology and crystallinity. Further high-resolution spectroscopy measurements are necessary for a conclusive assignment of the TL peaks to particular defects or centers.

Acknowledgements The authors acknowledge financial support from CONACYT grants nos. 83536 and 82765.

References

- [1] R. Chen and S. W. S. McKeever, *Theory of Thermoluminescence and Related Phenomena* (World Scientific, Singapore, 1997).
- [2] M. Benabdesselam, P. Iacconi, D. Briand, and J. E. Butler, *Diam. Relat. Mater.* **9**, 1013 (2000).
- [3] S. Mazzocchi, M. Bruzzi, M. Bucciolini, G. Cuttone, S. Pini, M. G. Sabini, and S. Sciortino, *Nucl. Instrum. Methods A* **476**, 713 (2002).

- [4] B. Marczewska, P. Olko, M. Nesladek, M. P. R. Waligorski, and Y. Kerremans, *Radiat. Prot. Dosim.* **101**, 485 (2002).
- [5] B. Marczewska, P. Bilski, M. Nesladek, P. Olko, M. Rebisz, and M. P. R. Waligorski, *Phys. Status Solidi A* **193**, 470 (2002).
- [6] J. Pospíšil, R. Bulf, Z. Budinská, R. Novák, B. Sopko, V. Spiváček, T. Čechák, P. Hlídek, P. Matějka, A. Macková, A. Cejnarová, and J. Krása, *Phys. Status Solidi A* **199**, 131 (2003).
- [7] M. Rebisz, M. J. Guerrero, D. Tromson, M. Pomorski, B. Marczewska, M. Nesladek, and P. Bergonzo, *Diam. Relat. Mater.* **13**, 796 (2004).
- [8] J. Krása, B. Marczewska, V. Vorlíček, P. Olko, and L. Juha, *Diam. Relat. Mater.* **16**, 1510 (2007).
- [9] S. Preciado-Flores, M. Schreck, R. Meléndrez, V. Chernov, R. Bernal, C. Cruz Vázquez, F. Brown, and M. Barboza-Flores, *Phys. Status Solidi A* **202**, 2206 (2005).
- [10] M. Barboza-Flores, M. Schreck, S. Preciado-Flores, R. Meléndrez, M. Pedroza-Montero, and V. Chernov, *Phys. Status Solidi A* **204**, 3047 (2007).
- [11] M. Benabdesselam, P. Iaconi, D. Briand, D. Lapraz, and J. E. Butler, *Radiat. Prot. Dosim.* **84**(1–4), 257, (1999).
- [12] B. Marczewska, C. Furetta, P. Bilski, and P. Olko, *Phys. Stat. Sol. (A)* **185**, 183 (2001).
- [13] J. Pospíšil, R. Novák, B. Sopko, V. Spiváček, P. Hlídek, P. Matějka, A. Macková, A. Cejnarová, L. Juha, and J. Krása, *Phys. Status Solidi A* **185**, 195 (2001).
- [14] C.-C. Liu, J.-P. Lin, and T.-C. Chu, *Appl. Radiat. Isot.* **59**, 79 (2003).
- [15] J. Krása, L. Juha, V. Vorlíček, and A. Cejnarová, *Nucl. Instrum. Methods, A* **524**, 332 (2004).
- [16] E. Borch, M. Bruzzi, C. Leroy, and S. Sciortino, *J. Phys. D, Appl. Phys.* **31**, 609 (1998).
- [17] F. Bogani, E. Borch, M. Bruzzi, C. Leroy, and S. Sciortino, *Nucl. Instrum. Methods Phys. Res. A* **388**, 427 (1997).
- [18] M. Benabdesselam, B. Serrano, P. Iaconi, F. Wrobel, D. Lapraz, J. Heralult, and J. E. Butler, *Radiat. Prot. Dosim.* **120**, 87 (2006).
- [19] M. Benabdesselam, P. Iaconi, J. E. Butler, and D. Briand, *Diam. Relat. Mater.* **10**, 2084 (2001).
- [20] C. Descamps, D. Tromson, M. J. Guerrero, C. Mer, E. Rzepka, M. Nesladek, and P. Bergonzo, *Diam. Relat. Mater.* **15**, 833 (2006).
- [21] C. Descamps, D. Tromson, C. Mer, M. Nesladek, P. Bergonzo, and M. Benabdesselam, *Phys. Status Solidi A* **203**(12), 3161 (2006).
- [22] M. Benabdesselam, P. Iaconi, D. Briand, D. Lapraz, E. Gheeraert, and A. Deneuille, *Diam. Relat. Mater.* **9**, 56 (2000).
- [23] A. J. Eccles, T. A. Steele, A. Afzal, C. A. Rego, W. Ahmed, P. W. May, and S. M. Leeds, *Thin Solid Films* **343**, 620 (1999).
- [24] P. W. May, P. R. Burrige, C. A. Rego, R. S. Tsang, M. N. R. Ashfold, K. N. Rosser, R. E. Tanner, D. Cherns, and R. Vincent, *Diam. Relat. Mater.* **5**, 354 (1996).
- [25] D. Briand, P. Iaconi, M. Benabdesselam, D. Lapraz, P. W. May, and C. A. Rego, *Diam. Relat. Mater.* **9**, 1245 (2000).
- [26] D. Briand, P. Iaconi, M. Benabdesselam, D. Lapraz, R. Bindi, P. W. May, C. A. Rego, and A. Afzal, *Thin Solid Films* **359**, 150 (2000).
- [27] H. Calvo del Castillo, J. L. Ruvalcaba, E. Belmont, T. Calderón, R. Meléndrez, and M. Barboza-Flores, *Phys. Status Solidi A* **205**, 2221 (2008).
- [28] A. M. Zaitsev, *Optical Properties of Diamond: A Data Handbook* (Springer, Berlin, 2001).
- [29] C. Manfredotti, in: *Carbon, The Future Material for Advanced Technology Applications, Topics in Applied Physics Vol. 100*, edited by G. Messina, and S. Santangelo (Springer, Berlin, Heidelberg 2006), p. 239.
- [30] M. Benabdesselam, P. Iaconi, J. E. Butler, and J. M. Nigoul, *Diam. Relat. Mater.* **12**, 1750 (2003).
- [31] E. Cruz-Zaragoza, R. Meléndrez, V. Chernov, M. Barboza-Flores, and S. Gastéum, *Nucl. Instrum. Methods B* **248**, 103 (2006).